A combined nonlinear and nonlocal model for topographic evolution in channelized depositional systems

F. Falcini,[1,2] E. Foufoula-Georgiou,[1,3] V. Ganti,[1,3,4] C. Paola,[1,5] and V. R. Voller[1,3]

Received 6 July 2012; revised 8 July 2013; accepted 9 July 2013.

[1] Models for the overall topographic evolution of erosional and depositional systems can be grouped into two broad classes. The first class is local models in which the sediment flux at a point is expressed as a linear or nonlinear function of local hydrogeomorphic measures (e.g., water discharge and slope). The second class is nonlocal models, where the sediment flux at a point is expressed via a weighted average (i.e., convolution integral) of measures upstream and/or downstream of the point of interest. Until now, the nonlinear and nonlocal models have been developed independently. In this study, we develop a unified model for large-scale morphological evolution that combines both nonlinear and nonlocal approaches. With this model, we show that in a depositional system, under piston-style subsidence, the topographic signatures of nonlinearity and nonlocality are identical and that in combination, their influence is additive. Furthermore, unlike either nonlinear or nonlocal models alone, the combined model fits observed fluvial profiles with parameter values that are consistent with theory and independent observations. By contrast, under conditions of steady bypass, the nonlocal and nonlinear components in the combined model have distinctly different signatures. In the absence of nonlocality, a purely nonlinear model always predicts a bypass fluvial profile with a spatially constant slope, while a nonlocal model produces a nonconstant slope, i.e., profile curvature. This result can be used as a test for inferring the presence of nonlocality and for untangling the relative roles of local and nonlocal mechanisms in shaping depositional morphology.

Citation: Falcini, F., E. Foufoula-Georgiou, V. Ganti, C. Paola, and V. R. Voller (2013), A combined nonlinear and nonlocal model for topographic evolution in channelized depositional systems, *J. Geophys. Res. Earth Surf.*, *118*, doi:10.1002/jgrf.20108.

1. Introduction

[2] There is a wide range of problems in river morphodynamics and landscape evolution where simple relationships between averaged sediment flux and averaged drivers, such as topography, sediment properties, and water discharge, provide useful predictive models, especially over large space and/or time scales. Because the flow is fundamentally gravity driven, relations of this kind are often cast in a form in which the flux is a function of the topographic slope. Although there have been numerous analyses proposing different ways to relate flux to topographic slope [*Paola*, 2000], until recently, there was little question that the slope to use in such models was the one at the point of interest. This view, however, has been challenged in a series of recent papers [e.g., *Bradley et al.*, 2010; *Foufoula-Georgiou et al.*, 2010; *Ganti et al.*, 2010; 2011; *Ganti*, 2012; *Schumer et al.*, 2009; *Stark et al.*, 2009; *Voller and Paola*, 2010; *Voller et al.*, 2012], which propose that in some cases the sediment flux at a point might also depend on values of the slope (or other topographic measures) away from that point. This dependence, typically expressed via some form of convolution integral, i.e., weighted average over space and/or time, takes into account the fact that probabilistic sediment motion may span a wide range of transport length scales. One end-member case is when the sediment motion exhibits a probability distribution with a power-law decaying tail ("heavy tail"). In this case, it is not possible to assign a characteristic length scale of transport [e.g., *Benson*, 1998] and consequently rigorous descriptions of macroscale morphologic evolution are best cast in terms of the so-called fractional calculus [e.g., *Podlubny*, 1999; *Foufoula-Georgiou et al.*, 2010; *Furbish and Haff*, 2010; *Ganti et al.*, 2010; *Ganti*, 2012; *Schumer et al.*, 2009; *Voller and Paola*, 2010].

[3] The idea that system evolution at a point also depends on conditions away—potentially quite far away—from that point is referred to as "nonlocality". Conceptually, it

[1]St. Anthony Falls Laboratory and National Center for Earth-Surface Dynamics, University of Minnesota, Minneapolis, Minnesota, USA.
[2]Istituto di Scienze dell'Atmosfera e del Clima, Consiglio Nazionale delle Ricerche, Rome, Italy.
[3]Department of Civil Engineering, University of Minnesota, Minneapolis, Minnesota, USA.
[4]Division of Geological and Planetary Sciences, California Institute of Technology, Pasadena, California, USA.
[5]Department of Earth Sciences, University of Minnesota, Minneapolis, Minnesota, USA.

Corresponding author: V. R. Voller, St. Anthony Falls Laboratory, Department of Civil Engineering, University of Minnesota, 2 3rd Ave SE, Minneapolis, Minnesota 55455, USA. (volle001@umn.edu)

2169-9003/13/10.1002/jgrf.20108

represents a profound shift in thinking about how influence and information are distributed and propagated in landscapes. So one might well ask: Exactly what difference does nonlocality make to overall morphologic evolution? Clearly, it is easy to see how a model using a nonlocal flux formulation could produce a much wider range of behavior outcomes (e.g., anomalous diffusion [*Chaves*, 1998; *Metzler and Klafter*, 2000]) when compared to a model that uses a standard linear diffusion treatment in which the flux is proportional to the local slope. It has been observed, however [*Foufoula-Georgiou et al*., 2010; *Voller and Paola*, 2010], that more general, but still local, flux models based on a nonlinear function of the local slope also allow for prediction of a wide set of behaviors, many of which partially or completely replicate the macroscopic behaviors arising from nonlocality. If this is so, then do we really need nonlocality?

[4] One answer is that if the underlying transport process is really nonlocal, representing the effects of that process via a contrived nonlinearity is likely to be prone to error, continual tuning, and scale dependence of the tuned parameters [e.g., *Ganti et al*., 2012]. More fundamentally, *any* local model implies that two points with the same local slope, water discharge, etc. would yield the same sediment flux, no matter where these points sit in the landscape relative to their upstream and downstream conditions. Is this really reasonable?

[5] As discussed earlier, nonlocal transport formulations are often associated with the absence of a characteristic scale of transport as manifested, for example, in power-law probability distributions of sediment travel distances (often truncated at the scale of the system). One sufficient but not necessary condition for such power-law distributions is the presence of a "transport network" or collection of pathways that exhibits fractality or internal self-similarity, e.g., the self-similar geometry of drainage networks [*Rinaldo and Rodriguez-Iturbe*, 1996], braided rivers [e.g., *Sapozhnikov and Foufoula-Georgiou*, 1996; 1999; *Foufoula-Georgiou and Sapozhnikov*, 1998; 2001; *Sapozhnikov et al*., 1998], and delta distributaries [*Wolinsky et al*., 2010; *Edmonds et al*., 2011]. If, to first order, we think of fluvial systems as comprising a network of efficient sediment transport pathways (channels and channel segments) and resting places (e.g., floodplains and bars), then the fractal geometry of the channel network system suggests a broad range of transport speeds, across multiple space and time scales. Thus, fractal geometry of the transport system leads naturally to a power-law distribution of transport steps. The fractal geometry of channels in a braided river system, for example, should result in sediment motions that span a wide range of spatiotemporal scales, and thus themselves exhibit heavy-tailed distributions. The occurrence of such heavy-tailed motions is a fundamental requirement for nonlocal transport [e.g., *Ganti*, 2012; *Ganti et al*., 2010; *Schumer et al*., 2009], raising the possibility that nonlocality could be a common, intrinsic feature of channelized transport systems.

[6] The potential influence of nonlocal transport on understanding the workings of channelized systems goes beyond simply describing the evolution of topographic profiles. For example, *Voller et al*. [2012] recently showed that nonlocality leads directly to a fundamental consequence for how topographic information propagates in landscapes: purely downstream in erosional systems and purely upstream in depositional systems. We stress that this is a statement only about how influence flows in space; the particles themselves, of course, move downstream. The applicability of insights like this depends on knowing to what extent nonlocal as opposed to nonlinear effects govern transport behavior in landscapes.

[7] To this end, untangling the effects of nonlocal versus nonlinear sediment transport dynamics has been difficult because the two approaches have been mutually exclusive. Our primary aim here is to bridge this gap by developing a combined nonlocal, nonlinear (NLNL) framework for the topographic evolution of fluvial systems. Our study highlights the important distinctions and similarities between the topographic signatures of nonlinear and nonlocal sediment transport dynamics, and we hope that it will provide insight and further impetus for more precise experiments that will allow us to explore unambiguously the presence and the relative role of nonlinearity and nonlocality in depositional systems.

2. Background on Nonlinear and Nonlocal Approaches

[8] We focus on the one-dimensional problem of evolution of a river long profile over time scales that average many individual flood events and space scales many times greater than a characteristic channel width. Under these conditions, in a long profile with downstream direction x and fluvial elevation above a datum $h(x)$, a straightforward means of capturing the relation between sediment flux q and topography is to set the sediment flux proportional to the negative of the local topographic gradient, viz., $q = -\nu\,\partial h/\partial x$, where ν is an appropriately adjusted constant diffusivity. Since this relationship relates flux to a potential gradient, it is often referred to as a linear diffusion flux model.

[9] In many cases a simple linear diffusion model for the sediment flux may not be adequate. For example, in a steady state ($\partial h/\partial t = 0$) depositional system subjected to a subsidence rate $\sigma(x)$, solutions of the governing Exner mass balance equation

$$\frac{d}{dx}(q) = \sigma, \tag{1}$$

using a linear diffusion model, often result in predictions of d^2h/dx^2—loosely referred to as the profile curvature—inconsistent with those observed in nature or laboratory experiments. In particular, as discussed in detail in *Voller and Paola* [2010], predictions of experimental depositional systems, based on linear diffusive fluxes, persistently suggest downstream fluvial curvature values in excess of those observed; typically the predicted curvature is positive, whereas the observed value is closer to zero (i.e., a straight line).

[10] One approach for dealing with deviations from simple linear diffusion behavior, such as this "curvature anomaly", is to use a nonlinear diffusion model that relates the flux to a power n of the fluvial slope; such models have been used in a number of studies that describe fluvial transport in depositional systems [e.g., *Postma et al*., 2008; *Swenson and Muto*, 2007; *Lorenzo-Trueba and Voller*, 2010]. In essence, noting that typical surfaces in depositional systems are concave up, such an approach works since—in the transient

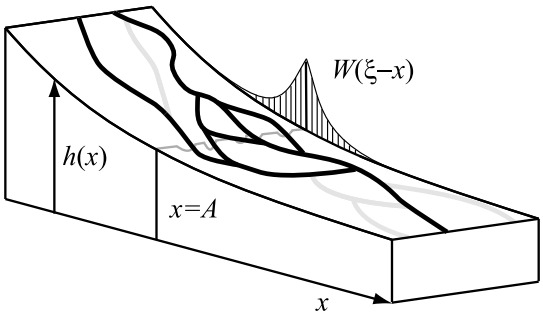

Figure 1. Schematic of a fluvial surface. Nonlocality arises because the sediment flux at a given point x = *A* is influenced by transport paths of a wide range of lengths (indicated by the black paths in the channel network). In a nonlocal setting, the sediment flux at $x = A$ is thus controlled by the properties remote from this point. A general nonlocal model of the flux can be formulated as a power-law weighted sum of functions of hydrogeomorphic measures throughout the domain; the figure indicates how such weights decay as we move away from the point $x = A$.

development of a given surface—the appearance of regions of high fluvial curvatures (high local changes in slope) would be counteracted by a local increase in sediment supply. This form of flux model, however, raises a potential inconsistency. Theoretical analysis, based on combining standard sediment flux relationships with flow and momentum balance [*Paola et al*., 1992; *Lai and Capart*, 2007; *Swenson et al*., 2000; *Lorenzo-Trueba et al*., 2009; *Postma et al*., 2008], leads to exponent values in the range $1 \le n \le 1.66$. This is in contrast to reported fits to experimental observations [*Swenson and Muto*, 2007; *Parker et al*., 2007; *Parker and Muto*, 2003; *Postma et al*., 2008] that indicate higher values, in the range $1.95 < n < 3.2$.

[11] An alternative approach for dealing with the curvature anomaly starts from the case for nonlocality discussed above. Channel systems often exhibit a large range of heterogeneities and a space-time structure of transport pathways that lack a characteristic scale. In such cases, using a local sediment transport formulation is inconsistent with the geometry and dynamics of the system. A better, more general approach is then to model the flux at a given point as a weighted sum of an appropriate function of hydrogeomorphic measures (e.g., slope, discharge) taken over an area around the point of interest. A model like this is "nonlocal", and when used in the balance of equation (1), has been demonstrated to reproduce natural large-scale topography and reduce curvature anomalies [*Foufoula-Georgiou et al*., 2010; *Voller and Paola*, 2010; *Voller et al*., 2012].

[12] Both nonlinear and nonlocal sediment flux models appear able to explain natural topography. Should they then be viewed as alternative, competing theories of sediment transport, or as complementary theories? We view them as complementary, since both nonlinear and nonlocal mechanisms can act simultaneously on a landscape. Thus, our next step is to construct a general flux model that includes both nonlocal and nonlinear sediment transport dynamics. Though we focus on depositional and bypass systems, in principle, our approach could be applied to erosional systems as well.

3. A General Nonlocal Framework for Modeling Sediment Flux

3.1. The Notion of Nonlocal Transport

[13] We envision a general fluvial surface in which the x (downstream) direction is scaled to be between 0 and 1, where $x = 0$ is the input point for water and sediment (Figure 1). Our objective is to establish a 1-D sediment transport model for this surface. In a local treatment, our starting point is to assume that the flux at specific point $x = A$ can be expressed by a function (linear or otherwise) of local hydrogeomorphic measures (slope, discharge, etc.) at point A. The only spatial averaging permitted at A is in the cross-stream direction, i.e., normal to x. This lateral averaging, along with temporal averaging over many transport events, then results in evaluation of the local average flux, which is then a function of x [see *Paola et al*., 1992]; we label this flux $q \equiv q^L(x)$.

[14] To build a general nonlocal flux treatment, we also account for hydrogeomorphic measures at points upstream and downstream of $x = A$ [*Voller et al*., 2012; *Furbish and Roering*, 2013]. A convenient and general means of achieving this is to define the nonlocal flux in terms of the convolution integral

$$q(x) = \int_0^1 W(x,\xi) q^L(\xi)\, d\xi, \tag{2}$$

where $W(x,\xi)$ are appropriate weights and in this general case $q^L(x)$ is a reference flux whose physical interpretation requires some care. It is a function of hydrogeomorphic measures associated with the transect at location x, as opposed to the actual flux that would be measured at that position. The measured flux at position x reduces to $q^L(x)$ in two specific cases: in a purely local treatment or the special case of nonlocal transport where the transport is spatially uniform and attention is restricted to a region sufficiently distant from the domain boundaries. Hence, equation (2) represents a weighted integral (convolution) of the reference flux $q^L(x)$ over the entire domain of interest. As noted in the Introduction, there are a variety of conditions and processes that would imply nonlocality. Possible examples include, but are not limited to, channel network patterns that naturally exhibit a wide range of transport length scales (e.g., the power-law distributions of stream lengths and island sizes found in deltas and braided rivers) and heterogeneous sediment production and transport (including erosion, slope failures, channel avulsions, and sediment trapping) that induce, at any point in the landscape, a broad range of entrainment and deposition probabilities.

[15] As written, equation (2) is a general definition of a nonlocal flux. Equation (2) is connected to physical systems in three ways: first, through the specification of the arguments (i.e., local hydrogeomorphic measures like slope, water discharge, etc.) of the function $q^L(x)$, second, through the form of this function (e.g., nonlinear versus linear), and third, through specification of the weights. In the following, we explore how these definitions and specifications can be made.

3.2. A Local Process Model

[16] To move forward, we narrow our choice of local hydrogeomorphic measures to the topographic slope. In this

way, for the specific case when $q^L(x)$ is a linear function of this slope, the nonlocal framework in equation (2) will be consistent with previous fractional calculus models of nonlocality [*Foufoula-Georgiou et al*., 2010; *Voller and Paola*, 2010; *Voller et al*., 2012]. Given that our goal is to develop a combined nonlocal, nonlinear model, our next step is, through the use of basic sediment transport relations and reasonable physical assumptions, to arrive at a general *local*, nonlinear sediment transport model in terms of the topographic slope. Nonlocal effects will then be represented through the weights in equation (2). The development of the nonlinear sediment flux model follows the ideas and concepts found in previous works [*Lorenzo-Trueba et al*., 2009; *Swenson et al*., 2000].

[17] We start with the classic bed load sediment transport equation due to *Meyer-Peter and Müller* [1948], which relates a dimensionless sediment transport rate q^L to a dimensionless shear stress τ acting in the fluvial channels on depositional surface, viz.,

$$q^L \sim (\tau - \tau_c)^{3/2}, \tag{3}$$

where τ_c is the critical shear stress at which bed load transport is initiated. Two common field cases are of interest. In gravel bed rivers, the channel width self-adjusts to keep the bed shear stress slightly above critical, $\tau = (1+\varepsilon)\tau_c$ [*Parker*, 1978; *Parker et al*., 2007]. Alternatively, in sand and fine-grained channels, $\tau >> \tau_c$ [*Dade and Friend*, 1998; *Parker et al*., 1998]. In both these cases equation (3) can be simplified to the form [*Paola et al*., 1992; *Paola*, 2000]

$$q^L \sim \tau^{3/2}. \tag{4}$$

[18] In contrast, considering the total bed material load—the sum of the bed load and the bed material part of the suspended load—the sediment transport rate can be modeled by the *Englund and Hansen* [1967] relation of form

$$q^L \sim \tau^{5/2}. \tag{5}$$

[19] Together, while not universal, equations (4) and (5) suggest that a reasonable general form for the sediment transport rate follows

$$q^L \sim \tau^m, \quad \frac{3}{2} \le m \le \frac{5}{2}. \tag{6}$$

[20] On using conservation of fluid mass, assuming that the momentum balance reduces to $\tau = -\rho g h\, dh/dx$, (where ρ is fluid density and g is gravitational acceleration) and adopting a standard quadratic drag law to represent the shear stress (i.e., $\tau = C_f U^2$, where C_f is a friction coefficient and U the depth-average fluid velocity), it can also be shown—see details in *Lorenzo-Trueba et al*. [2009] and *Swenson et al*. [2000]—that

$$\tau \sim \left[-\frac{dh}{dx}\right]^{\frac{2}{3}}. \tag{7}$$

Combining equations (6) and (7) leads to a general nonlinear local flux model

$$q^L = v\left|\frac{dh}{dx}\right|^{n-1}\left[-\frac{dh}{dx}\right], \quad n \ge 1. \tag{8}$$

[21] Within this basic theory, the exponent n in equation (8) is in the range $1 \le n \le 1.66$. As noted in the Introduction, this is inconsistent with experimental observations that place the exponent in the range $1.95 < n < 3.2$ [*Swenson and Muto*, 2007; *Parker et al*., 2007; *Parker and Muto*, 2003; *Postma et al*., 2008]. To account for this difference, *Postma et al*. [2008] suggest that neglecting the critical shear stress may not always be valid, presenting analysis to show that, in some systems, accounting for the critical shear stress leads to values of n well within the experimental range. We note, however, that some of the experiments used to determine the value of n involve relatively fine sediments and flow scenarios in which the shear stress is significantly larger than the threshold shear stress, a situation consistent with the simplified theoretical treatment. For example, in analyzing a flume/sediment system similar to the one used in *Swenson and Muto* [2007], *Parker and Muto* [2003], and *Lorenzo-Trueba et al*. [2009, *Lorenzo-Trueba and Voller*, 2010] show that the applied shear stress was up to 21 times larger than the threshold shear stress. Hence, the explanation proposed by *Postma et al*. [2008] seems inapplicable to some of the cases where the inferred exponent in the transport model is out of the range suggested above. This motivates us to ask whether nonlocal effects could account for the apparent difference between theoretical and experimental values of the nonlinearity exponent n.

[22] To help ease our later analysis, we define a nonlinearity parameter

$$\beta \equiv \frac{1}{n} \tag{9}$$

and we restrict attention to systems where the fluvial surface elevation $h(x)$ decreases monotonically in the downstream direction. The first step means that we measure nonlinearity on a 0 to 1 scale; the second means that we avoid the awkward calculus associated with taking absolute values. As such, our working model for the local flux is in the form

$$q^L(x) = v\left(-\frac{dh}{dx}\right)^{n-1}\left(-\frac{dh}{dx}\right) \equiv v\left(-\frac{dh}{dx}\right)^{\frac{1}{\beta}-1}\left(-\frac{dh}{dx}\right),$$
$$0 > \beta \ge 1, n \ge 1. \tag{10}$$

[23] We emphasize that in a purely local model, equation (10) would be the measured average sediment flux at location x, i.e., $q \equiv q^L(x)$, whereas in a nonlocal treatment, $q^L(x)$ would be a reference sediment flux for location x.

3.3. Nonlocal Weighting

[24] In essence, a sediment mass balance model represents the balance of fluxes into and out of a region of the landscape—a detailed discussion of such a flux balance can be found in *Paola and Voller* [2005]. The central element in these models is an appropriate representation of the sediment flux at a given location. Here, through our general equation (2), we are proposing a representation that couples the two concepts for sediment flux models that form the basis of this paper:

The first uses our understanding of fluvial sediment transport processes to relate the flux to functions of local fluvial hydrogeomorphic measures as embodied in the nonlinear flux model in equation (10). The second concept is the influence of nonlocal effects—that is, the representative flux at a given point can be partially controlled by landscape features or events remote from that point. With reference to equation (2), the specific realization of a nonlocal model comes about from specification of the weights $W(x,\xi)$. In developing such a realization, it is important to recognize that nonlocality by its nature reflects the influence of multiple processes occurring across a wide range of space and time scales. Although useful explanations of specific nonlocal mechanisms have been proposed [*Furbish and Roering*, 2013], the range of potential processes contributing to nonlocal transport is quite broad. Hence, at this point of our understanding, we think there is merit in developing *phenomenological*, nonlocal treatments through the identification of simple rules for determining the weights in equation (2). Testing alternative models of this nature against physical observations will inform our developing understanding of what nonlocality and locality are and how they might operate in the landscape.

[25] As an aside, to provide a historical context and justification, we note that when Henry Darcy proposed his equation to describe infiltration in the Dijon sandstones [*Darcy*, 1856], it was for all essential purposes a phenomenological model that fitted the observed data. It was not until fairly recently, through the application of extensive theory [*Whitaker*, 1985], that a connection between Darcy's simple law and the governing equations of the flow in the pores of a medium was established.

[26] Coming back to the task at hand, obvious requirements in a phenomenological nonlocal approach are that the weights $W(x,\xi)$ (1) cannot be negative, (2) must decrease in value with increasing distance from x, and (3) should have an integral over the domain of order 1. Within these basic rules, however, we have some choice. An important selection in this regard is the domain of the integral in equation (2), which can be viewed as the region about the point x that influences that point. It is the region over which the weights $W(x,\xi)$ are strictly positive. Since we know that the sediment moves on average downslope (downstream), an obvious and intuitive choice is to assume that the contributions to the nonlocality at point x are confined to points *upstream* of x. In this way, our general flux model would have the form

$$q(x) = \int_0^x W^u(x,\xi) q^L(\xi)\ d\xi. \tag{11}$$

[27] This is the form of nonlocal model used in modeling erosional hill slope domains [*Foufoula-Georgiou et al.*, 2010] so it certainly must be considered as a candidate nonlocal model for our present focus on depositional systems. However, that the sediment moves strictly downstream does not mean that influence flows strictly downstream. In previous theoretical work, *Voller et al.* [2012] showed that in application to closed depositional basins—where the positive input flux at $\xi = 0$ exactly balances a piston subsidence in $0 \le \xi \le 1$—equation (11) leads to physically implausible results. This is established through observing how a solution based on the upstream nonlocality in equation (11) satisfies the downstream flux boundary condition at $\xi = 1$, i.e., the condition that $q(1) = 0$. As we approach this boundary, $\xi \to 1$, (since all weights are considered to be nonzero) the only way to satisfy the boundary condition with the nonlocal definition equation (11) is to allow for the occurrence of negative nonlocal fluxes $q^L(\xi)$ somewhere in the domain [0, 1]. This in turn implies that sediment moves upstream! So while equation (11) is valid in some sediment transport systems, it is not universally so. This suggests that an alternative selection for the region of nonlocality contributions is to do the opposite of equation (11) and consider only contributions from the region downstream of x, i.e., set

$$q(x) = \int_x^1 W^d(x,\xi) q^L(\xi)\ d\xi. \tag{12}$$

[28] At first glance, it seems hard to imagine, given the prevailing flow of sediment, that the flux at a point is controlled by downstream events. We note, however, that the flows in many physical systems are controlled by downstream conditions, e.g., traffic flow upstream of a restriction such as a tunnel or lane closure [*Lighthill and Whitham*, 1955], and of course, in open channel hydraulics, the backwater control of upstream, subcritical flow by downstream obstacles. There are also examples in landscape dynamics where there is an upstream flow of "information", e.g., the upstream migration of meanders [*Zolezzi and Seminara*, 2001; *Zolezzi et al.*, 2005; *Seminara*, 2006], upstream migration of erosional fronts [*Tucker and Slingerland*, 1994], and upstream-propagating waves of deposition [*Hoyal and Sheets*, 2009]. Though these examples have not been framed in terms of nonlocality, they help highlight the key conceptual point, which is to distinguish the flow of material from the flow of influence or information.

[29] In light of the above, since we are primarily interested in applying our resulting model to study depositional systems, we will, in the first instance, restrict attention to the pure *downstream* nonlocality modeled by equation (12). In comparing with experimental data related to a zero-subsidence system, however, we also briefly investigate the upstream nonlocality of equation (11). This will clearly demonstrate that such an assumption does not lead to a satisfactory prediction of observed morphology.

[30] To proceed, we need to define explicitly the weights in equation (12). On assuming that the heterogeneity length scales that govern the nonlocality are power-law distributed through the fluvial domain [e.g., *Foufoula-Georgiou et al.*, 2010; *Ganti*, 2012], we can define appropriate (nonzero, monotonic) weights such that the *upstream* nonlocal model in equation (11) takes the form of the convolution integral

$$q^{non-loc-u} = \frac{1}{\Gamma(1-\alpha)} \int_0^x (x-\xi)^{-\alpha} q^L(\xi) d\xi, \tag{13}$$

and, in a similar manner, the *downstream* nonlocal model in equation (12) takes the form

$$q^{non-loc-d} = -\frac{1}{\Gamma(1-\alpha)} \int_x^1 (\xi-x)^{-\alpha} q^L(\xi) d\xi, \tag{14}$$

where $\Gamma(\cdot)$ is the gamma function. Providing a value of the nonlocality parameter $0 < \alpha \le 1$ in equations (13) and (14) gives us a degree of flexibility in specifying the nature of

our weights; note also that it can be shown that a value of $\alpha = 1$ reduces the flux definitions in equations (13) and (14) to be equivalent to a purely local flux at x.

[31] There are other advantages in our choice of weights. In particular, we note that with a linear definition for the reference flux, i.e., $q^L = -v\ dh/dx$, equations (13) and (14) can be respectively identified as the definitions for the left- and right-hand Caputo fractional derivatives [*Podlubny*, 1999]:

$$q^{non-loc-u} = -\frac{v}{\Gamma(1-\alpha)}\int_0^x (x-\xi)^{-\alpha}\frac{\partial h}{\partial \xi}d\xi, \tag{15}$$

$$q^{non-loc-d} = \frac{v}{\Gamma(1-\alpha)}\int_x^1 (\xi-x)^{-\alpha}\frac{\partial h}{\partial \xi}d\xi. \tag{16}$$

[32] Thus, by using the appropriate Laplace transform (see for example the appendix in *Voller and Paola* [2010]), we find that for a given real $\eta > \alpha$,

(i) if $h = x^\eta$

$$\frac{1}{\Gamma(1-\alpha)}\int_0^x (x-\xi)^{-\alpha}\frac{dh}{d\xi}d\xi = \frac{\Gamma(\eta+1)}{\Gamma(\eta+1-\alpha)}x^{\eta-\alpha}; \tag{17}$$

(ii) if $h = (1-x)^\eta$,

$$\frac{1}{\Gamma(1-\alpha)}\int_x^1 (\xi-x)^{-\alpha}\frac{dh}{d\xi}d\xi = \frac{\Gamma(\eta+1)}{\Gamma(\eta+1-\alpha)}(1-x)^{\eta-\alpha}. \tag{18}$$

[33] We finally point out that, in the context of a power-law distribution of heterogeneities, there is a strong assumption in choosing the weighting schemes in equations (15)–(18), viz., that the largest heterogeneity length scale in the system is of the same order as the domain size. When this is not the case, i.e., there is a clear scale separation between the domain size and the largest heterogeneity, we would expect any signal of nonlocality to be quenched. In other words, depending on the transport process and the heterogeneity length scales of a given system, the domain size itself might be a determining factor in choosing the weighting function.

4. A Steady State Model for Depositional Systems

[34] Following appropriate scaling, a simple but relevant test model for our proposed NLNL framework can be constructed by considering a steady state surface in a unit domain subjected to (1) no subsidence ($\sigma = 0$) [*Postma et al.*, 2008] or (2) a piston subsidence of unit magnitude ($\sigma = -1$) [*Voller et al.*, 2012]. From the Exner mass balance equation (1), the governing sediment transport equation for this system is

$$\frac{d}{dx}(q) = \begin{cases} 0, & \text{zero} \\ -1 & \text{piston} \end{cases} \qquad 0 \le x \le 1, \tag{19}$$

with boundary conditions

$$q(0) = 1, \quad h(1) = 0, \tag{20}$$

where q is the sediment flux defined by the nonlocal and/or nonlinear forms above.

5. Model Solutions

5.1. Local, Linear Diffusion

[35] In the case of a linear, local diffusive flux $q = -dh/dx$, where the constant diffusivity is taken equal to 1 for simplicity, it is easily verified through direct substitution that the solution of equations (19)–(20) is

$$h = \begin{cases} (1-x), & \text{zero} \\ \frac{1}{2}(1-x)^2, & \text{piston.} \end{cases} \tag{21}$$

5.2. Local, Nonlinear Diffusion

[36] The first step in obtaining a solution of equations (19) and (20), in the case where the sediment flux is given by the local, nonlinear form in equation (10), is to linearize the equation by setting

$$\left(-\frac{dh}{dx}\right)^{n-1}\left(-\frac{dh}{dx}\right) \equiv -\frac{d\gamma}{dx}, \tag{22}$$

where we simply substitute the product of the two terms in parentheses in equation (10) with a new derivative. Then, following from equation (21), the solution of equations (19)–(20) in terms of the new variable γ is

$$\gamma = \begin{cases} (1-x), & \text{zero} \\ \frac{1}{2}(1-x)^2, & \text{piston,} \end{cases} \tag{23}$$

thus allowing the right-hand side of equation (22) to be written as a function of x. The subsequent integration leads to the solution for the fluvial profile

$$h = \begin{cases} (1-x), & \text{zero} \\ \frac{n}{n+1}(1-x)^{1+\frac{1}{n}}, & n \ge 1, \quad \text{piston.} \end{cases} \tag{24}$$

[37] We note that when $n = 1$, this solution recovers the linear and local solution in equation (21) and that there is no signal of nonlinearity (i.e., no dependence on n) in the case of zero subsidence in the steady state profile. We also note that equation (24) can be reformulated in terms of $\beta = 1/n$ as

$$h = \begin{cases} (1-x), & \text{zero} \\ \frac{1}{1+\beta}(1-x)^{1+\beta}, & \text{piston.} \end{cases} \tag{25}$$

Table 1. Theoretical Values of the Shape Exponent of θ in Equation (32) for Difference Diffusion Flux Models and Subsidence Styles

Subsidence Style	Linear	Nonlinear	Nonlocal	NLNL
Zero	0	0	$\alpha-1$	$(\alpha-1)\beta$
Piston	1	β	α	$\alpha\beta$

[38] For our purposes, the above notation is more convenient since, unlike n, the parameter β is restricted to the interval (0, 1].

5.3. Nonlocal, Linear Diffusion

[39] If we assume that $q^L(\xi)$ has a linear dependence on the local topographic slope ($n=1/\beta=1$), we can use the fractional derivative results in equation (18) to verify that the fluvial profile solution to our test problems, when a downstream-directed nonlocality is present (flux model in equation (12)), is given by

$$h=\begin{cases}\dfrac{1}{\Gamma(\alpha+1)}(1-x)^{\alpha}, & \text{zero}\\[2ex] \dfrac{1}{\Gamma(\alpha+2)}(1-x)^{1+\alpha}, & \text{piston}\end{cases} \qquad 0<\alpha\le 1. \tag{26}$$

[40] We note that this result recovers the linear result in equation (21) when $\alpha=1$ and the piston solution in equation (26) matches the one previously obtained by *Voller and Paola* [2010]. In the case of piston subsidence, the nonlinear solution in equation (25) and the nonlocal solution in equation (26) have identical forms indicating that, with appropriately chosen parameters, both the nonlinear and downstream-directed nonlocal models have the *same* potential to match the curvature of observed depositional profiles.

6. The Nonlinear, Nonlocal (NLNL) Model

[41] Combination of the nonlinear and nonlocal models is readily achieved by simply using the nonlinear definition of q^L (equation (10)) in the *upstream* (equation (11)) or *downstream* (equation (12)) nonlocal models. This, for the downstream case, leads to the NLNL model

$$\begin{aligned} q^{NLNL} &= \frac{1}{\Gamma(1-\alpha)}\int_x^1 (\xi-x)^{-\alpha}\left(-\frac{dh}{d\xi}\right)^{n-1}\frac{dh}{d\xi}d\xi \\ &\equiv \frac{1}{\Gamma(1-\alpha)}\int_x^1 (\xi-x)^{-\alpha}\frac{d\gamma}{d\xi}d\xi, \end{aligned} \tag{27}$$

where the last term on the right-hand side arises from the linearization defined in equation (22). In this way, we see that the solution of equations (19) and (20), in terms of the linearized variable, γ, follows immediately from equation (26), i.e.,

$$\gamma=\begin{cases}\dfrac{1}{\Gamma(\alpha+1)}(1-x)^{\alpha}, & \text{zero}\\[2ex] \dfrac{1}{\Gamma(\alpha+2)}(1-x)^{1+\alpha}, & \text{piston}\end{cases} \qquad 0<a\le 1. \tag{28}$$

[42] When we substitute the above solution into equation (22), appropriate integration leads us to the following NLNL solution for the fluvial surface

$$h=\begin{cases}\dfrac{1}{1+\frac{\alpha}{n}-\frac{1}{n}}\left[\dfrac{\alpha}{\Gamma(\alpha+1)}\right]^{\frac{1}{n}}(1-x)^{1+\frac{\alpha}{n}-\frac{1}{n}}, & \text{zero}\\[2ex] \dfrac{n}{\alpha+n}\left[\dfrac{(1+\alpha)}{\Gamma(\alpha+2)}\right]^{\frac{1}{n}}(1-x)^{\frac{\alpha+n}{n}}, & \text{piston.}\end{cases} \tag{29}$$

[43] Or in terms of $\beta=1/n$,

$$h=\begin{cases}\dfrac{1}{1+\alpha\beta-\beta}\left[\dfrac{\alpha}{\Gamma(\alpha+1)}\right]^{\beta}(1-x)^{1+\alpha\beta-\beta}, & \text{zero}\\[2ex] \dfrac{1}{1+\alpha\beta}\left[\dfrac{(1+\alpha)}{\Gamma(\alpha+2)}\right]^{\beta}(1-x)^{1+\alpha\beta}, & \text{piston,}\end{cases} \tag{30}$$

where $0<\beta\le 1$, $0<\alpha\le 1$. The solutions in equation (30) represent a prediction for the steady state depositional profile that simultaneously accounts for both nonlocal and nonlinear dynamics in sediment transport. In particular, note that we recover (1) the linear solution when $\beta=\alpha=1$, (2) the nonlinear solution when $0<\beta<1$, $\alpha=1$, and (3) the nonlocal solution when $0<\alpha<1$, $\beta=1$.

[44] When the nonlocality is directed *upstream* (see equation (11)), a similar analysis leads to the zero-subsidence NLNL solution

$$h^{up}=\frac{1}{1+\alpha\beta-\beta}\left[\frac{\alpha}{\Gamma(\alpha+1)}\right]^{\beta}\left(1-x^{1+\alpha\beta-\beta}\right). \tag{31}$$

[45] This is almost identical in form to the *downstream* model solution (see first component of equation (30)) but with the exponent operating on x as opposed to $(1-x)$, a change that switches the sense of the fluvial curvature from concave down to concave up.

7. Analysis

[46] Before we present an experimental illustration of the operation of our proposed model via equation (30), it is worth investigating some of its consequences. In this respect, we note that all of the downstream nonlocality solutions have the generic forms

$$h=a(1-x)^{1+\theta} \tag{32}$$

where a is a constant and the exponent θ determines the resulting shape of the surface. Table 1 tabulates all of the forms of the shape exponent θ. The key conclusion is that the degree of nonlinearity is always biased by the presence and level of nonlocality. The way in which this bias operates, however, depends on the contrasting subsidence styles. In the case of piston subsidence, the exponent in all models has the same form and in the NLNL case the nonlinear and nonlocal parameters contribute multiplicatively to the exponent, i.e., $\theta=\alpha\beta$. As such, we note that, in matching a given value of θ, an increase in the nonlocality (a decrease in the value of α) requires a reduction in the level of nonlinearity (an increase

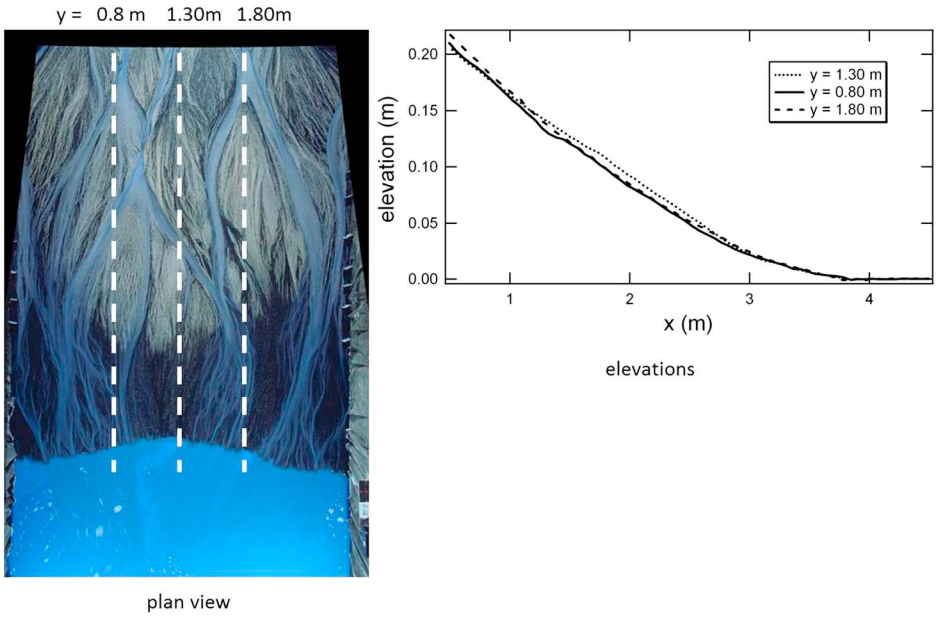

Figure 2. Experimental fluvial profiles in a depositional system; on the left, the fluvial surface plan view and, on the right, elevation of the profiles along different transects. Note this figure is taken from Figure 1 in *Voller and Paola* [2010] with the addition of the transect locations in the plan view and the subtraction of prediction in the elevation.

in the value of β). Hence, this behavior suggests that accounting for nonlocality in the system may allow for levels of nonlinearity $\beta = 1/n$ that fall within the theoretical range $1 \leq n \leq 1.66$.

[47] The zero-subsidence shape exponent reveals a different form of relationship between the nonlocality and nonlinearity. In particular, we note that in the absence of nonlocality (i.e., $\alpha = 1$), there is no signal of the nonlinearity in the steady state profile for zero subsidence, i.e., the profile becomes trivially linear (see equation (23)). It is only when nonlocality is present (i.e., $0 < \alpha < 1$) that curvature is induced and the signal of the nonlinearity revealed. This is an important observation because it suggests that the appearance of curvature in the steady, nonsubsiding fluvial profile indicates the presence of nonlocality, i.e., steady state profile curvature cannot be attributed to a nonlinear transport process alone. Further, in contrast to the piston subsidence case, the values of α and β in the zero-subsidence case do not counter one another in dictating the shape exponent. Indeed, for a given value of $-1 < \theta = (\alpha - 1)\beta < 0$, a decrease in α (an increase in nonlocality) also leads to a decrease in β (an increase in nonlinearity). In this way, the contrast in the nature of the fluvial shape exponent between the two subsidence styles provides a means—through experimentation on systems with controlled subsidence—of distinguishing and quantifying the degree of nonlocality and nonlinearity.

8. Experiment Illustrations of the NLNL Model

[48] The foregoing analysis of our combined NLNL model (equation (30)) suggests how the discrepancy between experimental and theoretically derived values of the nonlinear parameter $\beta = 1/n$ could be removed and how an observed fluvial profile might indicate the presence of nonlocality. To illustrate these features, here we fit our NLNL model to data obtained from fluvial profile experiments presented in the literature: a depositional system with subsidence investigated by *Voller and Paola* [2010] and a zero-subsidence depositional system reported by *Postma et al*. [2008]. We note that measurement noise, imperfect approach to steady state, and lack of complete knowledge of the entry and exit conditions, among other things, could in part obscure the signature of nonlinear and nonlocal sediment transport dynamics predicted by the proposed NLNL model. Nonetheless, this exercise still serves to illustrate how the NLNL model links—or should link—to physical systems and to show how more exact and definitive experiments for untangling nonlinear and nonlocal transport might be constructed.

[49] Data on deposition with subsidence [*Voller and Paola*, 2010] come from one of the Experimental Earthscape runs performed at Saint Anthony Falls Laboratory, University of Minnesota [*Kim et al*., 2006]. The experiment consists of supplying a mixture of quartz and anthracite sand (100–500 μm), to a tank (length 6 m, width 2.5 m) with a programmable subsiding floor. During the experiment, the supply rate of sediment is scaled to the rate of creation of volume by subsidence (accommodation), and the transport system organizes itself to deposit sediment to balance subsidence and maintain roughly consistent elevation, subject to external forcing. Figure 2 shows three experimental profiles from different downstream transects (indicated in the plan view photograph of the tank also shown in Figure 2). These profiles are from a period when the experiment was close to steady state, with the system running out of sand without a commensurate change in slope. The plan view of the experiment shows that this runout point is consistent during the period of interest; here we take a single representative value, 3750 mm. In order to compare this data with our NLNL model, we digitally

Table 2. Elevation for Subsidence Experiment Digitally Extracted from Figure 2

Downstream Position (mm)	Elevation (mm)		
	$y = 0.8$ m	$y = 1.3$ m	$y = 1.8$ m
500	208.33	205.00	217.08
750	187.50	186.67	191.67
1000	162.50	164.58	167.50
1250	137.50	145.83	142.50
1500	120.83	127.08	122.92
1750	100.83	112.50	100.83
2000	81.25	91.67	83.33
2250	66.67	73.75	66.67
2500	49.58	56.25	50.42
2750	32.92	37.50	37.50
3000	20.83	24.17	21.67
3250	12.50	12.50	12.50
3500	5.00	5.00	5.00

extracted the elevation profiles from Figure 2. The resulting profiles, with elevation every 250 mm, are given in Table 2 and plotted as symbols in Figure 3; the first downstream point we use is ~500 mm, a distance beyond the influence of perturbations associated with the sediment input. The form of NLNL to fit to these data is the second component of equation (30) written here as

$$h = A\left(1 - \frac{x}{3750}\right)^{1+\theta}, \quad \theta = \alpha\beta. \tag{33}$$

[50] We selected the parameters in this model to minimize the sum of squares for our extracted data points, i.e.,

$$SS = \sum_{\text{profile}} \sum_{k=1}^{3} \sum_{i=1}^{13} \left(h_i^k - h(x_i)\right)^2. \tag{34}$$

[51] The best fit line defined in this way, shown as a solid line in Figure 3, gives $A = 260$ and exponent $\theta = 0.47$. If we assume that nonlocality has no role in establishing this profile (i.e., $\alpha = 1$), this fit would suggest that our nonlinear exponent is $\beta = \theta = 0.47$, $(n = 2.13)$. This value is higher than the

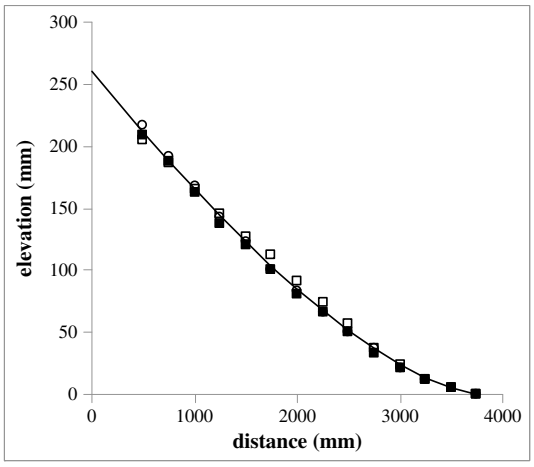

Figure 3. Plotting of experimental data in Table 2 (white squares: $y = 1.30$ m; circles: $y = 1.80$ m; black squares: $y = 0.80$ m) and best fit of NLNL model (solid line) $h = 260(1 - x/3750)^{1+0.47}$.

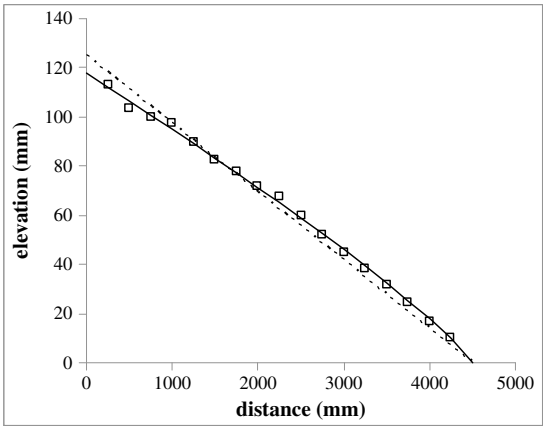

Figure 4. Plotting of experimental data in Table 3 (symbols), best fit NLNL model (solid line) $h = 118(1 - x/3750)^{1-0.14}$, and best fit linear (dashed line) $h = 124(1 - x/3750)$.

experimental value suggested by *Postma et al*. [2008], that is $\beta = 0.3125$, $(n = 3.2)$), but still 20% short of the expected lower theoretical limit $\beta = 0.6$, $(n = 1.67)$). This shortfall can, however, be mitigated if we allow for nonlocality in the system. In particular, since the exponent in the NLNL model is $\alpha\beta = \theta$, nonlocal exponents that satisfy $\theta \le \alpha \le 1.67$ will, for a given value θ, always result in a nonlinear exponent within the theoretical range $1 \le \beta \le 0.6$.

[52] As a further comparison, we turn to the zero-subsidence experimental data presented in *Postma et al*. [2008], which were digitally extracted from the near-steady state experimental profile reported in Figure 1 of their paper (squares in Figure 4; see Table 3 for list of the extracted data). The original experimental profile was arrived at by running a transient sand-sized deposition system to steady state, in a flume of length 4.5 m and width 0.11 m. Starting at $x = 250$ mm, we extracted data from this profile at intervals of $\Delta x = 250$ mm. As for the subsiding floor experiment, to reduce the impact of entry conditions, we chose the starting point for our data analysis a little away from the sediment input origin

Table 3. Elevation Data Extracted from Steady Sate Profile of Figure 1 in *Postma et al*. [2008]

Downstream Position (mm)	Elevation (mm)
250	112.83
500	103.50
750	100.00
1000	97.50
1250	89.67
1500	82.50
1750	77.50
2000	72.00
2250	67.50
2500	60.00
2750	52.00
3000	45.00
3250	38.33
3500	31.83
3750	24.50
4000	16.67
4250	10.17

$x = 0$. Here, with reference to the first component in equation (30), we fit the model

$$h = A\left(1 - \frac{x}{4500}\right)^{1+\theta}, \quad \theta = \alpha\beta - \beta. \tag{35}$$

[53] The best fit, shown as a solid line in Figure 4, has constant $A = 118$ and exponent $\theta = -0.14$. These choices generate a sum of squares of differences with the experiment data of $SS = 30$; as a point of contrast, the best linear ($\alpha = 1, \theta = 0, \ A = 124$) fit, shown as a dashed line in Figure 4, has a sum of squares $SS = 237$. As noted in our previous discussion, any negative nonzero exponent θ in equation (35), exhibited as a curved rather than a linear fluvial surface, indicates the presence of nonlocality. We do recognize that the observed curvature in this case is quite subtle. This could be attributed to the width of the flume (0.11 m), which may not allow for the full development of the channel network. We also recognize that there is some ambiguity in choosing experimental geometric parameters. To this last point, we note that (1) if we shift the first collected data point downstream from $x = 250$ mm to $x = 500$ mm, the best fit exponent value decreases slightly to $\theta = -0.143$ or (2) if we move back the projected end of the deposit from $x = 4500$ mm to $x = 4350$ mm, we decrease this exponent to $\theta = -0.21$. So we have a reasonably high degree of confidence that the extracted elevation data in Table 3 and Figure 4 demonstrate the appearance of nonlocality. Beyond this, the data also support the idea that in this system, built through depositional processes, the nonlocality is purely directed downstream.

[54] Although preliminary, the two example experimental data sets we have analyzed here also point toward a means by which we might be able (1) to justify the mutual presence of nonlocality and nonlinearity in depositional systems, and (2) to constrain an estimate of the nonlinear and nonlocal parameters β and α. Using the best fit values, the depositional experimental data imply

$$\alpha\beta = 0.47 \tag{36a}$$

and the bypass experimental data imply

$$\alpha\beta - \beta = -0.14. \tag{36b}$$

[55] Solution of the system (36) results in $\beta = 0.61$ and $\alpha = 0.77$, where the value of the nonlinear parameter is within the expected theoretical range $1 > \beta = 0.61 > 0.6$.

[56] In summary, we think that the two sets of experimental data used here, despite imperfections, meet our objectives of illustrating how nonlocality can modify the exponent in a nonlinear model and induce fluvial profile curvature in systems where local processes alone would predict none.

9. Conclusions

[57] The transport of sediment in the landscape is intrinsically nonlinear and, we argue, often intrinsically nonlocal. Our goal here has been to construct a framework for combining these two fundamental but previously disparate aspects of sediment transport dynamics: a unified nonlinear, nonlocal (NLNL) sediment flux model for prediction of river long profile evolution. On developing the NLNL model for systems with no subsidence and with piston-style subsidence, and comparing the model predictions with available experimental data for steady state depositional profiles, we conclude the following:

[58] 1. In combination, nonlinearity and nonlocality interact in ways that counterbalance one another in creating profile curvature for the piston subsidence case but oppose one another for the no subsidence case. Accounting for nonlocality in comparisons with experimental steady state fluvial profiles brings the best fit values of nonlinear parameters within the range of those expected from theoretical sediment transport arguments.

[59] 2. A concave fluvial profile formed in zero-subsidence experiments would unambiguously indicate the presence of nonlocality.

[60] 3. The ability of the proposed NLNL model to consistently reproduce experimental measurements from two independent systems provides support for the use of both nonlinear and nonlocal treatments in general sediment transport models.

[61] 4. Comparing subsiding and nonsubsiding steady state systems suggests a test by which nonlocal and nonlinear effects can be disentangled. The dependence of the interactions between the nonlocal and nonlinear components (competition versus amplification) due to the nature of the subsidence should allow for the construction of experiments that distinguish between the roles of nonlinearity and nonlocality in constructing topography.

[62] **Acknowledgments.** This work was supported by the STC program of the National Science Foundation via the National Center for Earth-Surface Dynamics under the agreement number EAR-0120914 and by the Flagship Project RITMARE to FF, funded by the Italian Ministry of Education, University and Research within the National Research Program 2011–2013. The authors are grateful for fruitful discussion and input from Roberto Garra and Alessandra Lanotte. The authors are also indebted to the editor Alexander Densmore, associate editor Dimitri Lague, and reviewers Nate Bradley, Philippe Davy, and David Furbish of the manuscript for providing informative and intellectually rich comments.

References

Benson, D. A. (1998), The fractional advection–dispersion equation: Development and application. PhD thesis, University of Nevada, Reno.

Bradley, D. N., G. E. Tucker, and D. A. Benson (2010), Fractional dispersion in a sand bed river, *J. Geophys. Res.*, *115*, F00A09, doi:10.1029/2009JF001268.

Chaves, A. S. (1998), A fractional diffusion equation to describe Lévy flights, *Phys. Lett. A*, *239*, 13–16.

Dade, W. B., and P. F. Friend (1998), Grain-size, sediment-transport regime, and channel slope in alluvial rivers, *J. Geol.*, *106*, 661–675.

Darcy, H. (1856), Determination of the laws of flow of water through sand (in French), in *Les Fontaines Publiquesd e la Ville de Dijon*, pp. 590–594, Victor Dalmont, Paris, (English translation, Physical Hydrogeology, edited by R. A. Freeze and W. Back, pp. 14–19, Van Nostrand Reinhold, New York, 1983).

Edmonds, D. A., C. Paola, D. C. J. D. Hoyal, and B. A. Sheets (2011), Quantitative metrics that describe river deltas and their channel networks, *J. Geophys. Res.*, *116*, F04022, doi:10.1029/2010JF001955.

Englund, F., and E. Hansen (1967), *A Monograph on Sediment Transport in Alluvial Streams*, 62 pp., Teknisk Forlag, Copenhagen, Denmark.

Foufoula-Georgiou, E., and V. B. Sapozhnikov (1998), Anisotropic scaling in braided rivers: An integrated theoretical framework and results from application to an experimental river, *Water Resour. Res.*, *34*(4), 863–867, doi:10.1029/98WR00216.

Foufoula-Georgiou, E., and V. Sapozhnikov (2001), Scale invariances in the morphology and evolution of braided rivers, *Mathematical Geology*, *33*(3), 273–291.

Foufoula-Georgiou, E., V. Ganti, and W. Dietrich (2010), A nonlocal theory of sediment transport on hillslopes, *J. Geophys. Res.*, *115*, F00A16, doi:10.1029/2009JF001280.

Furbish, D. J., and P. K. Haff (2010), From divots to swales: Hillslope sediment transport across divers length scales, *J. Geophys. Res.*, *115*, F03001, doi:10.1029/2009JF001576.

Furbish, D. J., and J. J. Roering (2013), Sediment disentrainment and the concept of local versus nonlocal transport on hillslopes, *J. Geophys. Res. Earth Surf.*, *118*, doi:10.1002/jgrf.20071.

Ganti, V. (2012), Non-local theories of geomorphic transport: From hillslopes to rivers to deltas to the stratigraphic record, PhD dissertation, 265 pp., University of Minnesota, Minneapolis, Minnesota.

Ganti, V., M. M. Meerschaert, E. Foufoula-Georgiou, E. Viparelli, and G. Parker (2010), Normal and anomalous diffusion of gravel tracer particles in rivers, *J. Geophys. Res.*, *115*, F00A12, doi:10.1029/2008JF001222.

Ganti, V., K. M. Straub, E. Foufoula-Georgiou, and C. Paola (2011), Space-time dynamics of depositional systems: Experimental evidence and theoretical modeling of heavy-tailed statistics, *J. Geophys. Res.*, *116*, F02011, doi:10.1029/2010JF001893.

Ganti, V., P. Passalacqua, and E. Foufoula-Georgiou (2012), A sub-grid scale closure for nonlinear hillslope sediment transport models, *J. Geophys. Res.*, *117*, F02012, doi:10.1029/2011JF002181.

Hoyal, D. C. J. D., and B. A. Sheets (2009), Morphodynamic evolution of experimental cohesive deltas. *J. Geophys. Res.*, *114*, F02009, doi:10.1029/2007JF000882.

Kim, W., C. Paola, V. R. Voller, and J. B. Swenson (2006), Experimental measurement of the relative importance of controls on shoreline migration, *J. Sediment. Res.*, *76*, 270–283, doi:10.2110/jsr.2006.019.

Lai, S. Y. J., and H. Capart (2007), Two-diffusion description of hyperpycnal deltas, *J. Geophys. Res.*, *112*, F03005, doi:10.1029/2006JF000617.

Lighthill, M. J., and G. B. Whitham (1955), On kinematic waves. II. A theory of traffic flow on long crowded roads, *Proceedings of the Royal Society A 229*, *317*, doi:10.1098/rspa.1955.0089.

Lorenzo-Trueba, J., and V. R. Voller (2010), Analytical and numerical solution of a generalized Stefan problem exhibiting two moving boundaries with application to ocean delta formation, *J. Math. Anal. Appl.*, *366*, 538–549.

Lorenzo-Trueba, J., V. R. Voller, T. Muto, W. Kim, C. Paola, and J. B. Swenson (2009), A similarity solution for a dual moving boundary problem associated with a coastal-plain depositional system, *J. Fluid Mech.*, *628*, 427–443.

Metzler, R., and J. Klafter (2000), The random walk's guide to anomalous diffusion: A fractional dynamics approach, *Phys. Rep.*, *339*, 1–77.

Meyer-Peter, E., and R. Müller (1948), Formulas for bed-load transport. Proceedings of the 2nd Meeting of the International Association for Hydraulic Structures Research. pp. 39–64.

Paola, C. (2000), Quantitative models of sedimentary basin filling, *Sedimentology*, *47*(suppl. 1), 121–178.

Paola, C., and V. R. Voller (2005), A generalized Exner equation for sediment mass balance, *J. Geophys. Res. 110*, F04014, doi:10.1029/2004JF000274.

Paola, C., P. L. Heller, and C. L. Angevine (1992), The large-scale dynamics of grain-size variation in alluvial basins, *Basin Res.*, *4*, 73–90.

Parker, G. (1978), Self-formed straight rivers with equilibrium banks and mobile bed. Part 2. The gravel river, *J. Fluid Mech.*, *89*, 127–146.

Parker, G., and T. Muto (2003) 1D numerical model of delta response to rising sea level, *Proceedings*, 3rd IAHR Symposium, River, Coastal and Estuarine Morphodynamics, Barcelona, Spain, 558–570.

Parker, G., C. Paola, K. X. Whipple, and D. C. Mohrig (1998), Alluvial fans formed by channelized fluvial and sheet flow. Part 1, *Theory. J. Hydraul. Engng*, *124*, 985–995.

Parker, G., P. R. Wilcock, C. Paola, W. E. Dietrich, and J. Pitlick (2007), Physical basis for quasi-universal relations describing bankfull hydraulic geometry of single-thread gravel bed rivers. *J. Geophys. Res. 112*, F04005. doi:10.1029/2006JF000549.

Podlubny, I. (1999), *Fractional Differential Equations*, Academic Press, New York.

Postma, G., M. G. Kleinhans, P. T. Meijer, and J. T. Eggenhuisen (2008), Sediment transport in analogue flume models compared with real world sedimentary systems: A new look at scaling sedimentary systems evolution in a flume, *Sedimentology*, *55*, 1541–1557.

Rinaldo, A., and I. Rodriguez-Iturbe (1996), The geomorphological theory of the hydrologic response, *Hydrol. Processes*, *10*(6), 803–829.

Sapozhnikov, V., and E. Foufoula-Georgiou (1996), Self-affinity in braided rivers, *Water Resour. Res.*, *32*, 1429–1439.

Sapozhnikov, V. B., and E. Foufoula-Georgiou (1999), Horizontal and vertical self-organization of braided rivers toward a critical state, *Water Resour. Res.*, *35*(3), 843–851, doi:10.1029/98WR02744.

Sapozhnikov, V. B., A. B. Murray, C. Paola, and E. Foufoula-Georgiou (1998), Validation of braided-stream models: Spatial state-space plots, self-affine scaling, and island shapes, *Water Resour. Res.*, *34*(9), 2353–2364, doi:10.1029/98WR01697.

Schumer, R., M. M. Meerschaert, and B. Baeumer (2009), Fractional advection-dispersion equations for modeling transport at the Earth surface, *J. Geophys. Res.*, *114*, F00A07, doi:10.1029/2008JF001246.

Seminara, G. (2006), Meanders, *J. Fluid Mech.*, *554*, 271–297.

Stark, C. P., E. Foufoula-Georgiou, and V. Ganti (2009), A nonlocal theory of sediment buffering and bedrock channel evolution, *J. Geophys. Res.*, *114*, F01029, doi:10.1029/2008JF000981.

Swenson, J. B., and T. Muto (2007), Response of coastal plain rivers to falling relative sea-level: Allogenic controls on the aggradational phase, *Sedimentology*, *54*, 207–221.

Swenson, J. B., V. R. Voller, C. Paola, G. Parker, and J. G. Marr (2000), Fluvio-deltaic sedimentation: A generalized Stefan problem, *Eur. J. Appl. Math.*, *11*, 433–452.

Tucker, G. E., and R. L. Slingerland (1994), Erosional dynamics, flexural isostasy, and long-lived escarpments: A numerical modeling study, *J. Geophys. Res.*, *99*, 12,229–12,243.

Voller, V. R., and C. Paola (2010), Can anomalous diffusion describe depositional fluvial profiles?, *J. Geophys. Res.*, *115*, F00A13, doi:10.1029/2009JF001278.

Voller, V. R., V. Ganti, C. Paola, and E. Foufoula-Georgiou (2012), Does the flow of information in a landscape have direction?, *Geophys. Res. Lett.*, *39*, L01403, doi:10.1029/2011GL050265.

Whitaker, S. (1985), Flow in porous media I: A theoretical derivation of Darcy's law, *Transport in Porous Media*, *1*, 3–25.

Wolinsky, M. A., D. A. Edmonds, J. Martin, and C. Paola (2010), Delta allometry: Growth laws for river deltas, *Geophys. Res. Lett.*, *37*, L21403, doi:10.1029/2010GL044592

Zolezzi, G., and G. Seminara, G. (2001) Downstream and upstream influence in river meandering. Part 1. General theory and application to overdeepening. *J. Fluid Mech.. 438*, 183–211.

Zolezzi, G., M. Guala, D. Termini, and G. Seminara (2005), Experimental observations of upstream overdeepening, *J. Fluid Mech.*, *531*, 191–219.